Gallego-Rodríguez, M.; Corma Canós, A.; Boronat Zaragoza, M. (2022). Influence of the zeolite support on the catalytic properties of confined metal clusters: a periodic DFT study of O2 dissociation on Cu-n clusters in CHA. Physical Chemistry Chemical Physics. 24(48):30044-30050. https://doi.org/10.1039/d2cp04915e

ARTICLE

Influence of the zeolite support on the catalytic properties of confined metal clusters: a periodic DFT study of O_2 dissociation on Cu_n clusters in CHA

Mario Gallego,[a] Avelino Corma[a] and Mercedes Boronat*[a]

The catalytic properties of sub nanometer Cu_n clusters are modified by interactions with the inorganic supports used for their stabilization. In this work the reactivity towards O_2 dissociation of Cu_5 and Cu_7 clusters confined within the cavities of CHA zeolite is theoretically investigated by means of periodic DFT calculations. Increasing the of Al content in the zeolite framework not only modifies cluster morphology, but also leads to a decrease in the electronic density available on the supported Cu_n clusters, which in turn leads to higher activation energies for O_2 dissociation. Together with cluster size and shape, the Si/Al ratio in the zeolite support appears as a potential parameter to finely tune the stability and oxidation properties of Cu-based catalysts.

Introduction

Sub nanometre metal clusters composed by just a few atoms exhibit electronic, optical, and catalytic properties different from those of larger nanoparticles and bulk metals, which are mostly associated to the accessibility of their low coordinated atoms and to a molecular-like electronic structure with discrete energy levels and localized orbitals. The catalytic properties of metal clusters depend strongly on their size and shape, and are altered by interactions with protecting ligands or inorganic supports. Understanding the nature and extent of these modifications is key to potentially achieve a fine tuning of their catalytic performance.[1-8] Copper is an abundant, cheap and nontoxic metal, so copper clusters are promising materials for various applications such as biosensors, therapeutic agents and efficient catalysts.[9-11] Previous theoretical and experimental work in our group has demonstrated that the ability of copper clusters to dissociate O_2, and the subsequent reactivity of the resulting adsorbed O atoms, is closely linked to the size and morphology of the cluster. The activation energy for O_2 dissociation on planar (2D) Cu_5 clusters is much higher than on 3D Cu_5 or Cu_7 clusters, making them more resistant against oxidation.[12,13] Moreover, the reactivity of bi-coordinated O atoms adsorbed at the edges of planar (2D) Cu_5 clusters is different from that of O atoms three-coordinated on Cu facets, with direct implications in the reaction mechanism and selectivity achieved in propene epoxidation, CO oxidation, and partial methane oxidation to methanol.[14-16]

For practical application, it is necessary to stabilize metal clusters either with protecting ligands in solution or by supporting them on solid organic or inorganic matrices, which could provoke changes in their electronic structure and therefore modify their catalytic behaviour. Graphene-based materials, metal-organic frameworks (MOFs), metal oxides and microporous solids have been used as supports for metal nanoparticles and clusters,[2, 4-8,17-26] and there are numerous examples where the behaviour of the metal is modified due to the interaction with the support. Thus, strong interactions between Cu clusters and perovskite support were theoretically and experimentally confirmed in $Cu_2O_n/SrTiO_3$ nanocomposite catalysts for CO oxidation and NO reduction;[22] enhanced activity and improved stability for low T CO oxidation were reported for calcined Cu clusters supported on CeO_2 nanorods;[23] the amount of highly dispersed Cu^0 and Cu^+ species necessary to catalyze the Water Gas Shift reaction was optimized in Cu/SiO_2 catalyst;[24] the catalytic performance of Cu/ZrO_2 catalysts in the CO_2 hydrogenation to methanol was enhanced by increasing the number of Cu-ZrO_2 interface sites;[25] and even the crystallographic phase of ZrO_2 in Cu/ZrO_2 catalysts was found to influence the formation of acetaldehyde and ethyl acetate from ethanol.[26] It seems therefore necessary to understand at a molecular level the nature of the interactions between metal clusters and supports.

Zeolites are good candidates to investigate the influence of the support on the electronic and catalytic properties of metal clusters. On one hand, their microporous structure composed by Si and O atoms provides an excellent environment to confine small metal clusters and prevent their agglomeration into larger particles. On the other hand, the substitution of Si atoms with Al in the framework generates a net negative charge that must be compensated with species bearing positive charge, such as protons, isolated cations or partially charged metal clusters.[17-21] By modifying the amount of Al in the zeolite framework it is possible to modulate the total positive charge on the confined metal clusters, and analyse how this factor affects their reactivity.

In this contribution, we explore by means of periodic density functional (DFT) calculations whether the trends previously reported for O_2 dissociation on copper clusters are modified when the clusters are confined within the cavities of a zeolite with the CHA structure (see Figure 1). For this purpose, we consider three different clusters, planar Cu_5-2D, three-dimensional Cu_5-3D and three-dimensional Cu_7-3D, stabilized within the cages of CHA models containing an increasing amount of framework Al atoms (nAl = 0, 1 and 2). Then, we investigate the adsorption and dissociation of molecular O_2 on each of the nine resulting Cu_n-CHA systems using dispersion-corrected DFT calculations, and analyse the possible correlations between optimized geometry, charge transfer and activation energy barriers. We find that the presence of Al atoms in the zeolite framework modifies the geometrical structure and the ability of the supported Cu_n clusters to dissociate O_2, making them more resistant against oxidation and good candidates for challenging oxidation reactions at experimentally significant Si/Al ratios.

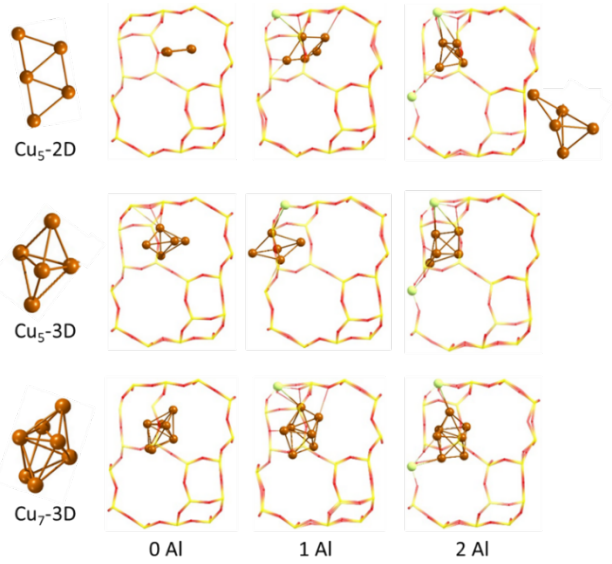

Figure 1. Optimized structures of Cu_5-2D, Cu_5-3D and Cu_7-3D clusters, isolated and confined within CHA models containing 0, 1 and 2 framework Al atoms. Si and O are depicted as red and yellow wires, Cu and Al are depicted as brown and light green balls.

Experimental

Periodic density functional theory (p-DFT) were performed using the VASP 5.2 code[27,28] and the PBE functional[29] including Grimme's D3 correction[30] for dispersion interactions. The valence density was expanded in a plane wave basis set with a kinetic energy cutoff of 600 eV, and the effect of the core electrons in the valence density was taken into account by means of the projected augmented wave (PAW) formalism.[31] All calculations are spin-polarized, and in all cases all structures converged to a doublet state with only one unpaired electron. Electronic energies were converged to 10^{-6} eV and geometries were optimized until forces on atoms were <0.01 eV/A. Integration in the reciprocal space was carried out at the Γ k-point of the Brillouin zone.

The zeolite chabazite, with the CHA structure, was modelled by means of a hexagonal unit cell with lattice with parameters a = b = 13.8026 Å, c = 15.0753 Å, α = β = 90° and γ = 120°, containing 36 T atoms (Si or Al) and 72 O atoms. Three zeolite framework compositions with increasing number of Al atoms (nAl = 0, 1 and 2) and three copper clusters with different size and morphology, (Cu_5-2D, Cu_5-3D and Cu_7-3D), were considered, giving rise to nine different catalytic systems. For each system, the copper cluster was initially placed in the centre of the CHA cage and in the proximity of the 8-ring window connecting two cages. Figure 1 shows the most stable structures obtained after geometry optimization.

In all calculations, the positions of all atoms in the system were fully optimized without restrictions. Transition states were characterized by frequency calculations to confirm that the imaginary frequency corresponds to the desired reaction coordinate. The Hessian matrix and vibrational frequencies were calculated using density functional perturbation theory (DFPT).[32] Transition states were located using the DIMER algorithm.[33,34] Atomic charges were calculated using the NBO approach.[35] The MOLDEN[36] and ChemCraft[37] programs were used throughout the work to visualize the systems and their frequencies.

Results and discussion

Confined Cu_n clusters

Figure 1 shows the most stable isomers of isolated Cu_5-2D, Cu_5-3D and Cu_7-3D, together with their optimized geometries when they are confined within the cavities of CHA models containing 0, 1 and 2 framework Al atoms. Interaction of Cu_n clusters with the pure silica CHA framework (0Al model) is weak and does not lead to any relevant geometry deformation of the confined clusters. The shortest Cu-O_f distances are 2.387, 2.097 and 2.281 Å in Cu_5-2D, Cu_5-3D and Cu_7-3D, respectively, and the three clusters become positively charged by less than 0.2 e (see Table 1). The substitution of one Si atom by Al (1Al model) generates a net negative charge in the zeolite framework that is compensated by the appearance of a positive charge of ~0.8 e on the confined clusters (see Table 1). The shortest Cu-O_f distances in the 1Al model decrease to 1.974 , 2.067 and 2.125 Å in Cu_5-2D, Cu_5-3D and Cu_7-3D, and the planar geometry of the Cu_5-2D cluster is slightly distorted. When two Si atoms in the framework are replaced by Al (2Al model) all copper clusters interact strongly with the framework, forming at least 6 bonds with the shortest optimized Cu-$O_{framework}$ distances being 1.984, 1.982 and 2.022 in Cu_5-2D, Cu_5-3D and Cu_7-3D, respectively. The positive charge in the clusters increases to ~1.5 e and, as in the case of 0Al and 1Al models, this positive charge is always largest on Cu_7-3D because of its larger number of electrons available to be transferred.

Table 1. Total atomic charges on Cu_n clusters (qCu_n, in e) and on adsorbed O_2 (qO_2, in e) calculated for the Cu_n clusters stabilized in CHA zeolite and for structures R, TS and P involved in O_2 dissociation.

	nAl	qCu_n catalyst	qCu_n (R)	qCu_n (TS)	qCu_n (P)
Cu_5-2D	0	0.167	0.918	1.442	2.169
	1	0.826	1.724	1.723	2.788
	2	1.510	2.158	2.655	3.354
Cu_5-3D	0	0.143	0.991	1.454	1.983
	1	0.785	1.966	2.139	2.507
	2	1.453	2.166	2.656	3.389
Cu_7-3D	0	0.205	1.217	1.414	2.181
	1	0.879	1.935	2.150	2.854
	2	1.549	2.496	2.768	3.327

O_2 adsorption on supported Cu_n clusters

Molecular O_2 adsorbs on small Cu_n clusters forming stable complexes in which the O-O bond is activated by charge transfer from the metal cluster to the π* orbital of O_2, facilitating its dissociation to produce adsorbed O atoms. In isolated clusters where all the electrons are available to be transferred the activation of molecular O_2 depends on the cluster size and on the geometry of adsorption on the cluster: the larger the number of Cu-O contacts, the larger the charge transferred to O_2.[9,10] When the clusters are supported in a zeolite the availability of electrons to be transferred decreases with increasing the Al content in the framework, adding a new variable to this process.

Figure 2 shows the optimized geometries of the most stable complexes found for O_2 adsorbed on Cu_5-2D, Cu_5-3D and Cu_7-3D clusters confined within CHA models containing 0, 1 and 2 framework Al atoms. Since these structures are the reactant species in the O_2 dissociation process, they are labelled as R in Tables 2 and 3, summarizing calculated charges and optimized OO bond lengths, respectively.

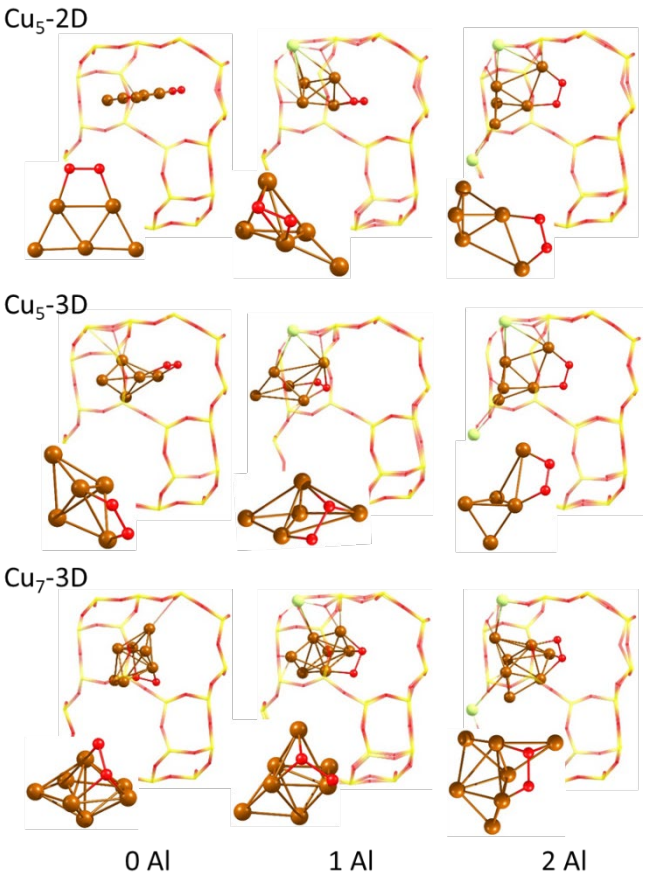

Figure 2. Optimized structures of O_2 adsorbed on Cu_5-2D, Cu_5-3D and Cu_7-3D clusters confined within CHA models containing 0, 1 and 2 framework Al atoms. Si and O are depicted as red and yellow wires, Cu and Al are depicted as brown and light green balls.

Table 2. Total atomic charges on adsorbed O_2 (qO_2, in e) calculated for structures R, TS and P involved in O_2 dissociation.

	nAl	qO_2 (R)	qO_2 (TS)	qO_2 (P)
Cu_5-2D	0	-0.858	-1.370	-2.101
	1	-1.000	-1.011	-2.070
	2	-0.741	-1.242	-1.986
Cu_5-3D	0	-0.913	-1.368	-1.983
	1	-1.208	-1.377	-1.773
	2	-0.732	-1.249	-2.016
Cu_7-3D	0	-1.065	-1.324	-2.075
	1	-1.171	-1.387	-2.087
	2	-1.036	-1.296	-1.894

Table 3. Optimized values of the OO distance (rOO, in Å) in structures R, TS and P involved in O_2 dissociation.

	nAl	rOO (R)	rOO (TS)	rOO (P)
Cu_5-2D	0	1.404	1.935	3.539
	1	1.468	1.883	3.616
	2	1.386	1.860	3.505
Cu_5-3D	0	1.422	1.852	3.551
	1	1.580	1.874	3.394
	2	1.383	1.872	3.421
Cu_7-3D	0	1.492	1.820	3.681
	1	1.565	1.932	3.650
	2	1.493	1.841	3.520

Molecular O_2 adsorbs on Cu_n clusters forming two or three Cu-O bonds. In the systems not containing Al the geometry of the cluster is not modified after O_2 adsorption, but in the 1Al and 2Al models the clusters undergo important restructuration upon interaction with O_2, usually leading to lower symmetry structures. The Cu_5-2D cluster loses its planarity and in the presence of two framework Al atoms it evolves to a 3D structure not too different from that obtained for Cu_5-3D cluster. In all cases a net transfer of electron density from the catalyst to O_2 occurs, leading to a net negative charge on adsorbed O_2 and a net positive charge on the Cu_n clusters that follows the trend with Al content reported for the confined clusters without adsorbates (see Tables 1 and 2, and Figure S1). However, not all the electron density lost by the metal clusters ends up in O_2 (see Figure S2). The largest capture of electron density by O_2 occurs in the systems with only one framework Al. Accordingly, the increase in the optimized O-O bond length is also largest in the 1Al models, and the correlation between rOO and neet charge on O_2 previously reported on isolated clusters is maintained here (see Figure 3a).The calculated adsorption energies E_{ads} summarized in Table 4 and plotted in Figure S3 are on average larger in the planar cluster Cu_5-2D than in Cu_5-3D and less favourable on Cu_7-3D, and as a general trend they are more favourable as the charge transferred to O_2 increases (see Figure 3b).

Table 4. Calculated adsorption (E_{ads}), activation (E_{act}) and reaction (ΔE) energies (in kJ/mol) for O_2 dissociation on Cu_n clusters stabilized in CHA.

	nAl	E_{ads}	E_{act}	ΔE
Cu_5-2D	0	-250	134	-230
	1	-181	46	-309
	2	-264	93	-235
Cu_5-3D	0	-186	50	-265
	1	-169	19	-176
	2	-204	99	-260
Cu_7-3D	0	-136	14	-289
	1	-193	31	-288
	2	-161	45	-260

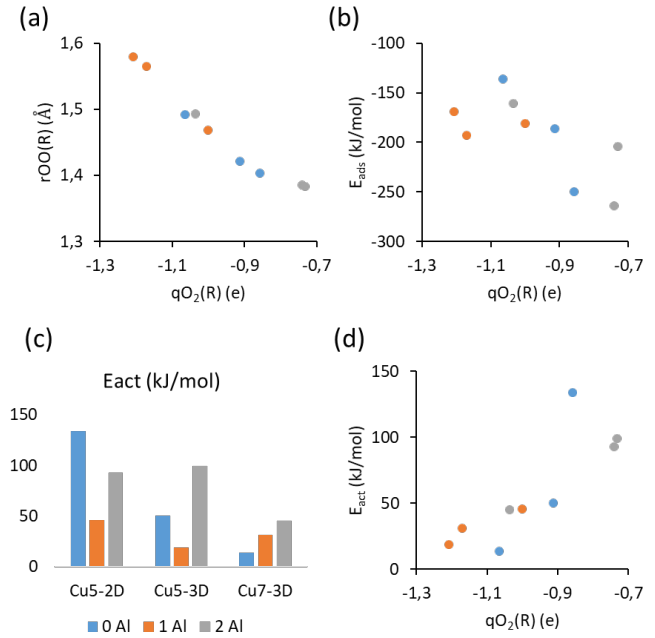

Figure 3. (a) Correlation between optimized OO bond length and total charge on O_2 in structures R. (b) Plot of calculated adsorption energy E_{ads} versus total charge on O_2 in structures R. (c) Activation energy for O_2 dissociation on Cu_n clusters. (d) Correlation between activation energy E_{act} and total charge on O_2 in structures R.

O_2 dissociation on supported Cu_n clusters

The electron density transferred to adsorbed O_2 weakens the OO bond facilitating its dissociation through the transition states depicted in Figure 4. The two O atoms are always interacting with at least two Cu atoms of the cluster, and the optimized OO distances in the TS structures range from 1.82 to 1.94 Å (see Table 3). Additional electron density is transferred to O_2 from the Cu_n clusters, whose positive charge increases following the trend with Al content described in Sections 3.1 and 3.2.

The activation energies for the dissociation of O_2 on the supported Cu_n clusters are summarized in Table 4 and plotted in Figure 3c to facilitate its analysis. In the systems without framework Al the trend in activation energies is quite similar to that previously reported for isolated clusters: high activation barriers for planar Cu_5-2D, that decrease when changing to 3D morphology (Cu_5-3D) and with increasing cluster size (Cu_7-3D). In the presence of framework Al atoms, the planar Cu_5-2D cluster rearranges upon interaction with O_2 adopting a 3D structure that, in turn, leads to a lower activation energy for O_2 dissociation. The three E_{act} values in the 1Al models are similar and really low, 46 and 19 kJ/mol for Cu_5 and 31 kJ/mol for Cu_7 (see Table 4). Finally, moving to the 2Al model with more positively charged Cu_n clusters results in an increase of all the calculated activation energies, more noticeable in the smaller Cu_5 clusters with less availability of electron density to activate O_2. As previously reported for isolated clusters,[12] there is a correlation between the calculated activation energies E_{act} and the total charge on O_2 in the reactant species R (see Figure 3d), suggesting that the degree of activation of the OO bond in adsorbed O_2 through electron density transfer to the π* anti-bonding orbital is what determines the energy that will be necessary to break this bond and dissociate molecular O_2.

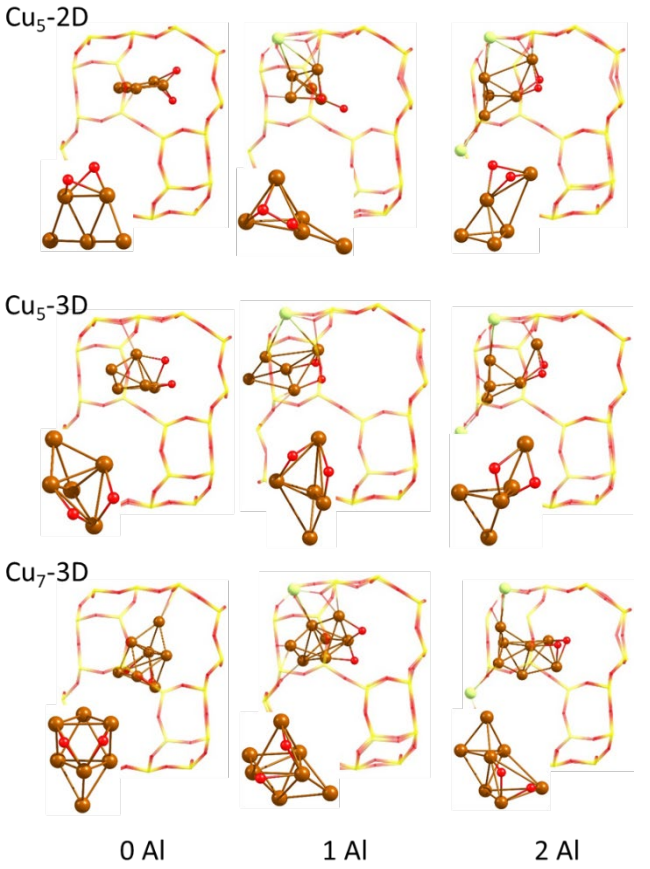

Figure 4. Optimized structures of the transition states for O_2 dissociation on Cu_5-2D, Cu_5-3D and Cu_7-3D clusters confined within CHA models containing 0, 1 and 2 framework Al atoms. Si and O are depicted as red and yellow wires, Cu and Al are depicted as brown and light green balls.

After dissociation, the two O atoms tend to occupy positions on the surface of the Cu_n clusters, either three-coordinated on the facets or bi-coordinated at the cluster edges (see Figure 5). The total positive charge on the Cu_n clusters increases to values between ~2.0 and ~3.4 e (see Table 1) and the adsorbed O atoms become negatively charged by ~ -1.0 e. The process is always clearly exothermic, with calculated reaction energies between -230 and -310 kJ/mol (ΔE values in Table 4). The only exception is the product of O_2 dissociation on the Cu_5-3D cluster supported on the 1Al zeolite model. The reaction energy is less favorable, -176 kJ/mol, and the net negative charge on the O atoms is also the lowest, -0.88 e on average on each atom. It could be related to the fact that after O_2 dissociation in this model the two O atoms are bi-coordinated at neighboring edges of the cluster sharing one Cu atom, which is a less stable situation than having at least one three-coordinated O atom as in all other cases (see amplified images in Figure 5).

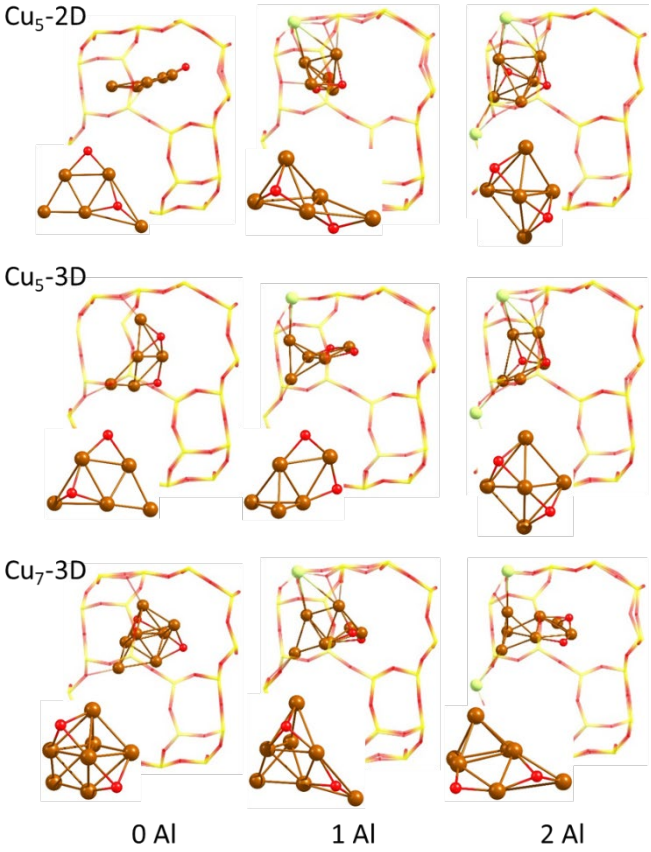

Figure 5. Optimized structures of two O atoms adsorbed on Cu_5-2D, Cu_5-3D and Cu_7-3D clusters confined within CHA models containing 0, 1 and 2 framework Al atoms. Si and O are depicted as red and yellow wires, Cu and Al are depicted as brown and light green balls.

Successive dissociation of multiple O_2 molecules on supported Cu_7

After the dissociation of the first O_2 molecule all clusters have increased significantly their positive charge, reaching values larger than 3.3 e in the systems with two framework Al atoms (see qCu_n (P) values in Table 1). Taking into account that electron density transfer to adsorbed O_2 is key to promote its dissociation, the possibility to avoid the undesired overoxidation of Cu_n clusters by supporting them on zeolites with the proper amount of Al was investigated. For this purpose, a second O_2 molecule was adsorbed on the product P structure obtained for Cu_7-3D, labelled Cu_7-3D-2O in Figure 7 and Table 5. As expected, less electron density is transferred to O_2 in this system, only -0.384 e (see Table 5), leading to a shorter optimized OO bond length, 1.388 Å, and to a higher activation energy for O_2 dissociation, 152 kJ/mol. This value is similar to that obtained for the planar Cu_5-2D cluster in the 0Al model, 134 kJ/mol, probably because of the similar geometry obtained for the adsorbed O_2 molecule at the edge of the cluster and for the transition state with the two O atoms sharing the same two Cu atoms forming the cluster edge (see Figure 6). In addition, at difference with all the other systems studied in this work, the dissociation of O_2 on the Cu_7-3D-2O cluster is endothermic by 63 kJ/mol, and the negative charge on the resulting adsorbed O atoms is small, ~-0.4 e.

To make this study systematic, the adsorption and dissociation of an O_2 molecule on Cu_7 clusters containing one, three and four additional O atoms, labelled Cu_7-3D-O, Cu_7-3D-3O and Cu_7-3D-4O in Figure S4 and Table 5, was also investigated. Again, the charge transferred to O_2 is less than -0.4 e, the optimized OO bond lengths are between 1.36 and 1.38Å, the calculated reaction energies are positive or only slightly negative, and the activation energies are higher than 100 kJ/mol with the only exception of the Cu_7-3D-4O system, probably due to the low stability of the reactant structure. These results indicate that deep oxidation of zeolite-supported Cu_n clusters by successive dissociation of O_2 molecules is disfavoured both kinetically and thermodynamically, making zeolites a promising support to stabilize metallic Cu.

Table 5. Total atomic charges on adsorbed O_2 (qO_2, in e) and optimized values of the OO distance (rOO, in Å) in structures R, TS and P involved in O_2 dissociation, and calculated adsorption (E_{ads}), activation (E_{act}) and reaction (ΔE) energies (in kJ/mol) for O_2 dissociation on Cu_7-3D clusters with increasing amount of adsorbed O stabilized in a CHA zeolite model with 2 framework Al atoms.

	Cu_7-3D	Cu_7-3D-O	Cu_7-3D-2O	Cu_7-3D-3O	Cu_7-3D-4O
qO_2 (R)	-1.036	-0.368	-0.384	-0.339	-0.355
qO_2 (TS)	-1.296	-0.654	-0.641	-0.584	-0.604
qO_2 (P)	-1.894	-0.924	-0.785	-0.889	-0.820
rOO (R)	1.493	1.383	1.388	1.368	1.359
rOO (TS)	1.841	1.830	1.916	1.893	1.649
rOO (P)	3.520	2.939	2.705	2.952	2.550
E_{ads}	-161	-283	-211	-287	-159
E_{act}	45	106	152	131	63
ΔE	-260	3	63	-18	-52

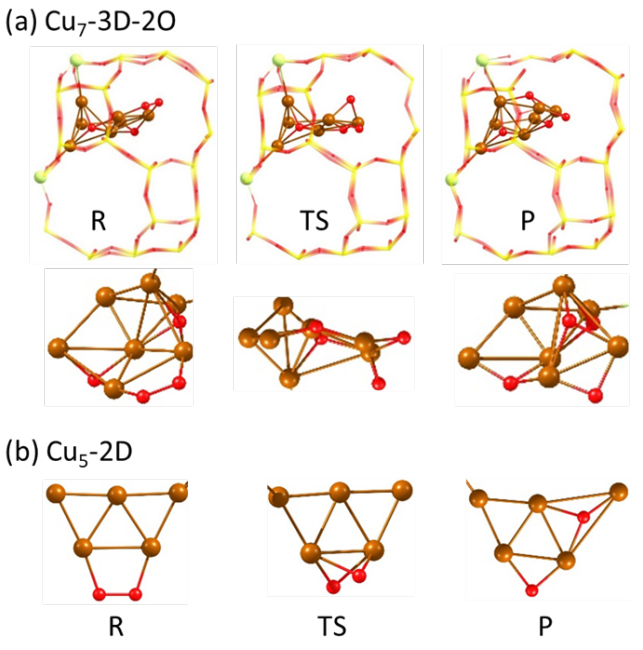

Figure 6. Optimized structures of reactant R, transition state TS and product P of O_2 dissociation reaction on (a) Cu_7-3D-2O in CHA with 2 framework Al and (b) Cu_5-2D clusters in CHA with 0 framework Al atoms. Si and O are depicted as red and yellow wires, Cu and Al are depicted as brown and light green balls.

Conclusions

The present computational study shows that the stabilization of Cu_n clusters within Al-containing zeolites modify their charge and morphology, and, as a consequence, their reactivity towards O_2. The

total positive charge on the Cu_n clusters increases with the number of Al atoms in the zeolite framework. O_2 adsorption and its subsequent dissociation into two O atoms requires an additional transfer of electron density from the catalyst to the O_2 and O species, leaving the Cu_n clusters highly charged after the reaction takes place. As a consequence, deep oxidation of zeolite supported Cu_n clusters by successive adsorption and dissociation of additional O_2 molecules is unlikely, which can be exploited to stabilize metallic oxidation state under oxidizing conditions, necessary for some challenging reactions.

Author Contributions

M. B. and A. C. directed the study. M. G. carried out the DFT calculations, supervised by M.B. All the authors discussed the results and contributed to the preparation, writing and revision of the manuscript.

Conflicts of interest

There are no conflicts to declare.

Acknowledgements

This work was supported by the Spanish Government through MCIN PID2020-112590GB-C21 and TED2021-130739B-I00 (MCIN/AEI/FEDER,UE). We thank Red Española de Supercomputación (RES) and Servei d'Informatica of the University of Valencia for computational resources and technical support. M. G. thanks the Spanish MCIN for his fellowship PRE2018-083547.

Notes and references

1 M. Boronat, A. Leyva-Pérez, A. Corma, *Acc. Chem. Res.,* 2014*,* **47**, 834.
2 L. Liu, A. Corma, *Chem. Rev.,* 2018*,* **118**, 4981.
3 K. Yamamoto, T. Imaoka, M. Tanabe, T. Kambe, *Chem. Rev.,* 2019, **120**, 1397.
4 E. Fernández, M. Boronat, *J. Phys.: Condens. Matter,* 2019*,* **31**, 013002.
5 Ch. Dong, Y. Li, D. Cheng, M. Zhang, J. Liu, Y. G. Wang, D. Xiao, D. Ma, *ACS Catal.,* 2020, **10**, 11011.
6 H. Rong, S. Ji, J. Zhang, D. Wang, Y. Li, *Nature Commun.,* 2021, **11**, 5884.
7 Serna, P.; Rodríguez-Fernández, A.; Yacob, S.; Kliewer, C.; Moliner, M.; Corma, A. Single-Site vs. Cluster Catalysis in High Temperature Oxidations, *Angew. Chem. Int. Ed.,* 2021, **60**, 15954.
8 F. Garnes-Portolés, R. Greco, J. Oliver-Meseguer, J. Castellanos-Soriano, M. C. Jiménez, M. López-Haro, J. C. Hernández-Garrido, M. Boronat, R. Pérez-Ruiz, A. Leyva-Pérez, *Nature Catal.,* 2021, **4**, 293.
9 A. Baghdasaryan T. Bürgi. Nanoscale, 2021, 13, 6283.
10 M. B. Gawande, A. Goswami, F. X. Felpin, T. Asefa, X. Huang, R. Silva, X. Zou, R. Zboril, R. S. Varma. Chem. Rev. 2016, 116, 3722.
11 Y. Yan, L. Ke, Y. Ding, Y. Zhang, K. Rui, H. Lin, J. Zhu. Mater. Chem. Front., 2021, 5, 2668.
12 E. Fernandez, M. Boronat, A. Corma, *J. Phys. Chem. C,* 2015, **119**, 19832.
13 P. Concepcion, M. Boronat, S. Garcia-Garcia, E. Fernandez, A. Corma, *ACS Catalysis*, 2017, **7**, 3560.
14 E. Fernandez, M. Boronat, A. Corma, *J. Phys. Chem. C,* 2020, **124**, 21549.
15 E. Fernández, M. Boronat, A. Corma. *Phys. Chem. Chem. Phys*., 2022, **24**, 4504.
16 M. Gallego, A. Corma, M. Boronat. *J. Phys. Chem. A* 2022, **126**, 4941.
17 P. del Campo, C. Martínez, A. Corma. *Chem. Soc. Rev.* 2021, **50**, 8511.
18 S. Grundne, M. A.C. Markovit, G. Li, M. Tromp, E. A. Pidko, E. J.M. Hensen, A. Jentys, M. Sanchez-Sanchez, J. A. Lercher. *Nat. Commun*. 2015**, 6**, 7546.
19 B. E. R. Snyder, M. L. Bols, R. A. Schoonheydt, B. F. Sels, E. I. Solomon. *Chem. Rev.* 2018, **118**, 2718.
20 M. H. Mahyuddin, Y. Shiota, A. Staykov, K. Yoshizawa. *Acc. Chem. Res.* 2018, **51**, 2382.
21 N. Kosinov, C. Liu, E. J. M. Hensen, E. A. Pidko. *Chem. Mater.*, 2018, **30**, 3177.
22 M. M. Natile, S. Carlotto, G. Bizzotto, A. Vittadini, A. Glisenti. *Eur. J. Inorg. Chem.* **2018**, 3829.
23 B. Wang, H. Zhang, W. Xu, X. Li, W. Wang, L. Zhang, Y. Li, Z. Peng, F. Yang,Z. Liu**.** *ACS Catal.* **2020**, 10, 12385.
24 C. Chen, H. Ren, Y. He, Y. Zhan, C. Au, Y. Luo, X. Lin, S. Liang, L. Jiang. *ChemCatChem* **2020**, *12*, 4672.
25 J. Yu, S. Liu, X. Mu, G. Yang, X. Luo, E. Lester, T. Wu. *Chem. Eng. J.* **2021**, 419, 129656.
26 A.G. Sato, D.P. Volanti, D.M. Meira, S. Damyanova, E. Longo, J.M.C. Bueno. *J. Catal.* **2013**, 307, 1.
27 J. Hafner. *J. Comput. Chem.* 2008, **29**, 2044.
28 G. Kresse, J. Furthmüller. *Phys. Rev. B* 1996, **54**, 11169.
29 J. P. Perdew, K. Burke, M. Ernzerhof. *Phys. Rev. Lett.* 1996, **77**, 3865.
30 S. Grimme, J. Antony, S. Ehrlich, H. Krieg. *J. Chem. Phys.* 2010, **132**, 154104.
31 P. E. Blöchl. *Phys. Rev. B* 1994, **50**, 17953.
32 S. Baroni, S. de Gironcoli, A. dal Corso, P. Giannozzi. *Rev. Mod. Phys.* 2001, **73**, 515.
33 G. Henkelman, H. Jonsson. *J. Chem. Phys.* 1999, **111**, 7010.
34 A. Heyden, A. T. Bell, F. J. Keil. *J. Chem. Phys.* 2005, **123**, 224101.
35 A. E. Reed, R. B. Weinstock, F. Weinhold. *J. Chem. Phys.* 1985, **83**, 735.
36 G. Schaftenaar, J. H. Nordik. *J. Comput. Aided Mol. Des.* 2000, ***14***, 123.
37 G. A. Adrienko. https://www.chemcraftprog.com.